Cancer Cell
Article

c-Raf, but Not B-Raf, Is Essential for Development of *K-Ras* Oncogene-Driven Non-Small Cell Lung Carcinoma

Rafael B. Blasco,[1,6] Sarah Francoz,[1,6] David Santamaría,[1] Marta Cañamero,[2] Pierre Dubus,[3] Jean Charron,[4] Manuela Baccarini,[5] and Mariano Barbacid[1,*]
[1]Molecular Oncology
[2]Biotechnology Programmes
Centro Nacional de Investigaciones Oncológicas (CNIO), E-28029 Madrid, Spain
[3]Université de Bordeaux, EA2406, F-33076 Bordeaux, France
[4]Centre de Recherche en Cancérologie de l'Université Laval, CRCHUQ, Hôtel-Dieu de Québec, Québec, QC G1R 2J6, Canada
[5]Max F. Perutz Laboratories, Center for Molecular Biology, University of Vienna, Vienna 1030, Austria
[6]These authors contributed equally to this work
*Correspondence: mbarbacid@cnio.es
DOI 10.1016/j.ccr.2011.04.002

SUMMARY

We have investigated the role of individual members of the Raf/Mek/Erk cascade in the onset of *K-Ras* oncogene-driven non-small cell lung carcinoma (NSCLC). Ablation of Erk1 or Erk2 in K-Ras oncogene-expressing lung cells had no significant effect due to compensatory activities. Yet, elimination of both Erk kinases completely blocked tumor development. Similar results were obtained with Mek kinases. Ablation of *B-Raf* had no significant effect on tumor development. However, c-Raf expression was absolutely essential for the onset of NSCLC. Interestingly, concomitant elimination of *c-Raf* and *B-Raf* in adult mice had no deleterious consequences for normal homeostasis. These results indicate that c-Raf plays a unique role in mediating K-Ras signaling and makes it a suitable target for therapeutic intervention.

INTRODUCTION

Ras proteins are small GTPases that serve as mitogenic switches to convey information generated at the cell surface to the nuclear transcriptional machinery through multiple effector cascades. These proteins have been extensively characterized at the structural, biochemical, and cellular level due to their central role in eukaryotic biology, as well as their implication in cancer development (Malumbres and Barbacid, 2003; Karnoub and Weinberg, 2008). To date, multiple Ras downstream effectors have been identified. It is generally accepted that the Raf/Mek/Erk cascade of kinases is the primary mediator of mitogenic activity (Marshall, 1994). Another well-known pathway, the PI3Kinase/Pdk/Akt pathway, is thought to mediate survival signals (Cully et al., 2006; Engelman et al., 2006). Other Ras effectors include the GDP/GTP exchange factors Tiam1 and RalGDS, which are responsible for activating other families of small GTPases involved in the control of cell polarity and motility as well as membrane trafficking (Malliri and Collard, 2003; Camonis and White, 2005). Other downstream effectors such as PLCe, AF6, Rin1, and RASSF have been less extensively characterized.

Despite this wealth of information, little is known about the precise pathways that mediate RAS oncogenic signaling in cancer. *K-RAS*, the *RAS* oncogene most frequently mutated in human cancer, has been implicated in a variety of tumor types including non-small cell lung carcinoma (NSCLC), one of the tumors with the worst prognosis and for which, to our knowledge, there are no effective treatments (Malumbres and Barbacid, 2003; Karnoub and Weinberg, 2008). Genetic studies in

Significance

K-RAS oncogenes have been implicated in one-fourth of non-small cell lung carcinomas (NSCLCs), one of the human tumors with the worst prognosis. Although K-RAS signals through a cascade of druggable kinases including the RAF, MEK1/2, and ERK1/2 kinases, to our knowledge, it is not known how these individual kinases contribute to tumor development. Here, we demonstrate that ablation of Mek1/2 or Erk1/2 kinases completely prevents tumor development, although their systemic elimination is incompatible with adult life. In contrast, ablation of c-*Raf* completely prevents *K-Ras*-driven NSCLC without inducing deleterious effects when systemically eliminated in adult tissues, either alone or in combination with B-*Raf*. These observations point to c-RAF as a suitable target for therapeutic intervention in *K-RAS*-driven NSCLC.

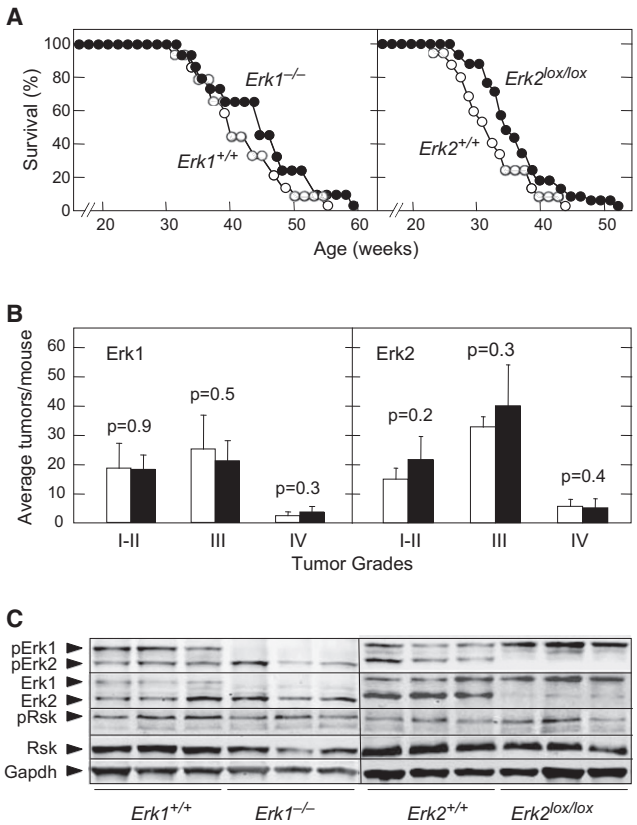

Figure 1. *K-Ras*^{G12V} Induces NSCLCs in the Absence of Erk1 or Erk2

(A) The left panel shows survival of *K-Ras*$^{+/G12V}$;*Erk1*$^{+/+}$ (n = 17) (open circles) and *K-Ras*$^{+/G12V}$;*Erk1*$^{-/-}$ (n = 14) (solid circles) mice treated with Ad-Cre at 8 weeks of age. The right panel illustrates survival of *K-Ras*$^{+/G12V}$;*Erk2*$^{+/+}$ (n = 19) (open circles) and *K-Ras*$^{+/G12V}$;*Erk2*$^{lox/lox}$ (n = 32) (solid circles) mice treated with Ad-Cre at 8 weeks of age.

(B) The left panel shows the number of tumors, classified by grade (I–IV), observed in *K-Ras*$^{+/G12V}$;*Erk1*$^{+/+}$ (n = 5) (open bars) and *K-Ras*$^{+/G12V}$;*Erk1*$^{-/-}$ (n = 5) (solid bars) mice sacrificed 6 months after Ad-Cre treatment. The right panel illustrates the number of tumors, classified by grade (I–IV), observed in *K-Ras*$^{+/G12V}$;*Erk2*$^{+/+}$ (n = 5) (open bars) and *K-Ras*$^{+/G12V}$;*Erk2*$^{lox/lox}$ (n = 5) (solid bars) mice sacrificed 6 months after Ad-Cre treatment. Error bars indicate mean ± SD. p values were calculated according to Student's t test.

(C) Western blot analysis of pErk1/2, Erk1/2, pRsk, and Rsk expression in lysates prepared from individual tumors of the indicated genotype collected 8 months after Ad-Cre treatment. Gapdh is shown as a loading control. Migration of the above proteins is indicated by arrowheads.

See also Figure S1.

mouse models of NSCLC (Johnson et al., 2001) have indicated that K-Ras may signal through the PI3Kinase/Akt pathway. Mice carrying a germline mutation in the alpha subunit of PI3Kinase that prevents interaction with Ras proteins developed significantly fewer lung tumors than control mice (Gupta et al., 2007). Ablation of the two loci encoding the p85 regulatory subunits of PI3Kinase also resulted in significant reduction of the number of tumors appearing in the same tumor model (Engelman et al., 2008). More recently, new therapeutic targets, including the NF-κB pathway and the cell cycle kinase Cdk4, have been identified by synthetic lethal approaches (Meylan et al., 2009; Puyol et al., 2010). Other potential targets identified by in vitro screens include the noncanonical IκB kinase, Tbk1, and the mitotic PLK1 kinase (Barbie et al., 2009; Luo et al., 2009). Interestingly, there is little information on the distinct contributions of the Raf/Mek/Erk kinases to *K-Ras*-induced NSCLC.

We undertook the present study to systematically examine by genetic means the contribution of the Raf/Mek/Erk cascade of kinases in a mouse model of *K-Ras*-driven NSCLC (Guerra et al., 2003). To this end, we have used strains of mice carrying mutations within *loci* encoding Raf, Mek, and Erk kinases to investigate whether they are essential for tumor development. The results described below provide information that might be used in the future to design targeted therapies to block *K-RAS*-induced NSCLC in human patients.

RESULTS

Elimination of Individual Erk Kinases Does Not Prevent *K-Ras*^{G12V}-Induced NSCLCs

We investigated whether the Erk kinases, Erk1 and Erk2, were necessary for the induction of NSCLC mediated by a resident *K-Ras*^{G12V} oncogene. *K-Ras*$^{+/LSLG12Vgeo}$ mice (designated from now on as *K-Ras*$^{+/G12V}$) (Guerra et al., 2003) were crossed to strains carrying mutated alleles of *Erk1* (*Erk1*$^{-/-}$) and *Erk2* (*Erk2*$^{lox/lox}$) (Pagès et al., 1999; Fischer et al., 2005). Eight-week-old *K-Ras*$^{+/G12V}$;*Erk1*$^{-/-}$ and *K-Ras*$^{+/G12V}$;*Erk2*$^{lox/lox}$ mice, along with control animals, were exposed by intratracheal instillation to replication-defective adenoviruses encoding the Cre recombinase (Ad-Cre). This strategy allowed expression of the resident K-Ras^{G12V} oncoprotein in the infected lung cells upon Cre-mediated recombination of the floxed stop cassette inserted within the *K-Ras* locus (Guerra et al., 2003). In addition the Cre recombinase also ablated the *Erk2*^{lox} alleles in those cells expressing the *K-Ras*^{G12V} oncogene.

Absence of either Erk1 or Erk2 resulted in limited increase of the lifespan of these animals (Figure 1A) . Whereas *K-Ras*$^{+/G12V}$;*Erk1*$^{+/+}$ mice (n = 17) displayed 50% survival at 40 weeks, *K-Ras*$^{+/G12V}$;*Erk1*$^{-/-}$ animals (n = 14) reached this survival rate at 46.3 weeks, a 20% increase taking into account that tumor development was initiated when mice were 8 weeks old. We obtained similar results when we ablated the locus encoding the Erk2 kinase. Ad-Cre treated *K-Ras*$^{+/G12V}$;*Erk2*$^{lox/lox}$ mice (n = 32) survived slightly longer than control *K-Ras*$^{+/G12V}$;*Erk2*$^{+/+}$ (n = 19) animals (50% survival at 34.9 versus 31.2 weeks, a 16% increase in survival) (Figure 1A). The difference in the time at which control mice reached 50% survival is due to the intrinsic variability of the different Ad-Cre preparations. Yet, because the same viral preparation was used for all mice in each experiment, the limited increase in survival observed in mice carrying the targeted *Erk* alleles must be attributable to the absence of the corresponding Erk kinase.

K-Ras$^{+/G12V}$;*Erk1*$^{-/-}$ and *K-Ras*$^{+/G12V}$;*Erk2*$^{lox/lox}$ mice sacrificed 6 months after Ad-Cre infection displayed tumor burden similar to those of control animals (Figure 1B). As expected, Erk1 was absent from *K-Ras*$^{+/G12V}$;*Erk1*$^{-/-}$ NSCLCs. Likewise, Erk2 could not be detected in lung tumors derived from *K-Ras*$^{+/G12V}$;*Erk2*$^{lox/lox}$ mice (Figure 1C) due to efficient excision of the *Erk2*^{lox} alleles (see Figure S1 available online). Absence of Erk1 or Erk2 did not result in increased expression of the

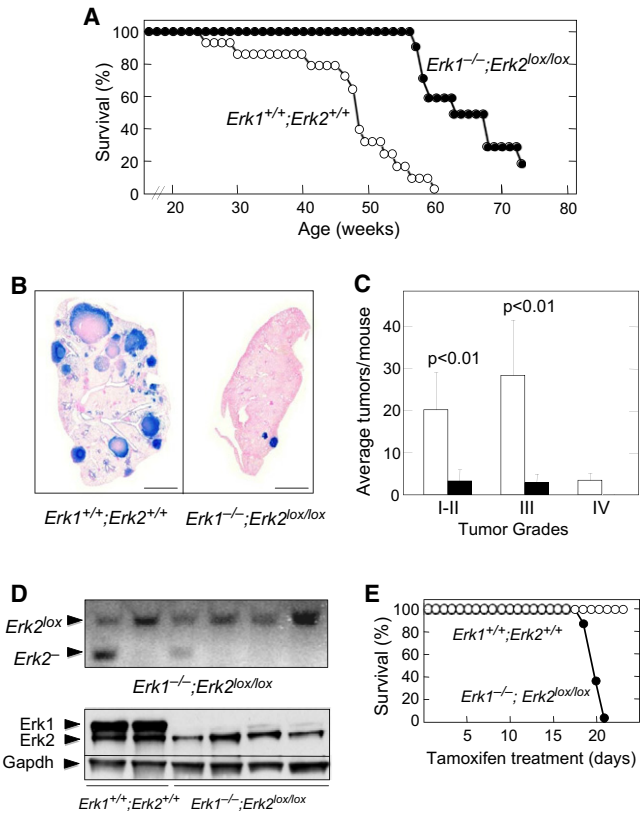

Figure 2. Complete Ablation of Erk1/2 Kinases Prevents Induction of NSCLCs by a Resident *K-Ras*^{G12V} Oncogene

(A) Survival of *K-Ras*$^{+/G12V}$;*Erk1*$^{+/+}$;*Erk2*$^{+/+}$ (n = 14) (open circles) and *K-Ras*$^{+/G12V}$;*Erk1*$^{-/-}$;*Erk2*$^{lox/lox}$ (n = 11) (solid circles) mice treated with Ad-Cre at 8 weeks of age.

(B) Whole-mount X-Gal staining of lung sections collected from mice with the indicated genotypes 6 months after Ad-Cre treatment. β-Geo positive cells identified by X-Gal staining (blue color) correspond to cells expressing K-Ras^{G12V}. Scale bars, 5 mm.

(C) Number of tumors, classified by grade (I–IV), observed in *K-Ras*$^{+/G12V}$;*Erk1*$^{+/+}$;*Erk2*$^{+/+}$ (n = 7) (open bars) and *K-Ras*$^{+/G12V}$;*Erk1*$^{-/-}$;*Erk2*$^{lox/lox}$ (n = 10) (solid bars) mice sacrificed 6 months after Ad-Cre treatment. Error bars indicate mean ± SD. p values were calculated according to Student's t test.

(D) The top panel shows Southern blot analysis of genomic DNA isolated from individual tumors of *K-Ras*$^{+/G12V}$;*Erk1*$^{-/-}$;*Erk2*$^{lox/lox}$ mice 8 months after Ad-Cre treatment. DNAs were digested with KpnI and probed with a 450 bp DNA fragment derived from the third intron just outside the floxed sequences. Migration of the unrecombined *Erk2*^{lox} allele (4.3 kbp) and the ablated *Erk2*$^{-}$ allele (2.4 kbp) is indicated by arrowheads. The bottom panel shows western blot analysis of Erk1 and Erk2 expression in lysates obtained from individual tumors collected 8 months after Ad-Cre treatment of *K-Ras*$^{+/G12V}$;*Erk1*$^{+/+}$;*Erk2*$^{+/+}$ and *K-Ras*$^{+/G12V}$;*Erk1*$^{-/-}$;*Erk2*$^{lox/lox}$ mice. The presence of Erk2 in tumors of Ad-Cre treated *K-Ras*$^{+/G12V}$;*Erk1*$^{-/-}$;*Erk2*$^{lox/lox}$ mice, due to incomplete cleavage of the *Erk2*^{lox} allele, indicates that Erk2 is essential for tumor development. Gapdh was used as loading control. Migration of the above proteins is indicated by arrowheads.

(E) Survival of *Erk1*$^{+/+}$;*Erk2*$^{+/+}$;*RERT*$^{ert/ert}$ (open circles) and *Erk1*$^{-/-}$;*Erk2*$^{lox/lox}$;*RERT*$^{ert/ert}$ (solid circles) mice fed ad libitum a tamoxifen-containing diet to activate the knocked in CreERT2 recombinase encoded by the *RERT*^{ert} alleles. See also Figure S2.

remaining kinase (Figure 1C). Likewise, the levels of pErk2 were the same in the presence or absence of Erk1, although the levels of pErk1 were slightly elevated in the absence of Erk2 (Figure 1C). Finally, the phosphorylation levels of Rsk, a well-known Erk downstream substrate, did not change upon elimination of either Erk1 or Erk2 (Figure 1C). These observations suggest that a single Erk kinase, either Erk1 or Erk2, is sufficient to process K-Ras^{G12V} oncogenic signaling to initiate NSCLC development.

Elimination of Erk1/2 Kinases Impairs Tumor Development and Induces Lethality in Adult Mice

To evaluate the effect of eliminating both Erk kinases in K-Ras^{G12V}-driven tumors, we generated *K-Ras*$^{+/G12V}$;*Erk1*$^{-/-}$;*Erk2*$^{lox/lox}$ mice and exposed their lungs to Ad-Cre infection. Control *K-Ras*$^{+/G12V}$;*Erk1*$^{+/+}$;*Erk2*$^{+/+}$ animals (n = 14) displayed a 50% survival at 48 weeks. Instead, the 50% survival point for *K-Ras*$^{+/G12V}$;*Erk1*$^{-/-}$;*Erk2*$^{lox/lox}$ mice (n = 11) was reached at 63 weeks (Figure 2A), thus representing a 40% increase in survival. When we examined *K-Ras*$^{+/G12V}$;*Erk1*$^{-/-}$;*Erk2*$^{lox/lox}$ mice 6 months after turning on K-Ras^{G12V} expression, we observed very few tumors compared to control animals (Figures 2B and 2C). More importantly, all tumors tested (n = 6) displayed a prominent band corresponding to the nonrecombined *Erk2*^{lox} allele and expressed normal levels of Erk2, indicating that these tumors were "escapers" (Figure 2D). These observations indicate that Erk2 is required for tumor development in the absence of Erk1.

Next, we examined whether Erk1/2 kinases might be required for normal homeostasis. To this end we generated *Erk1*$^{-/-}$;*Erk2*$^{lox/lox}$;*RERT*$^{ert/ert}$ mice. *RERT*^{ert} mice ubiquitously express an inducible CreERT2 recombinase (Guerra et al., 2003). Thirty-day-old *Erk1*$^{-/-}$;*Erk2*$^{lox/lox}$;*RERT*$^{ert/ert}$ mice were fed ad libitum with a tamoxifen-containing diet to systemically excise the *Erk2*^{lox} alleles. The health of these mice (n = 8) deteriorated rapidly, and all of them died within 3 weeks due to multiple organ failure (Figure 2E). DNA analysis of tissues obtained from moribund animals revealed recombination rates of the *Erk2*^{lox} alleles ranging from 40% to 60% (Figure S2). These observations indicate that loss of Erk proteins is incompatible with life in adult mice. Interestingly, preliminary results indicate that a single *Erk* allele is sufficient to maintain adult homeostasis because *Erk1*$^{-/-}$;*Erk2*$^{+/lox}$;*RERT*$^{ert/ert}$ (n = 2) and *Erk1*$^{+/-}$;*Erk2*$^{lox/lox}$;*RERT*$^{ert/ert}$ (n = 3) mice exposed to a tamoxifen diet for 3 months did not show significant abnormalities (data not shown).

Individual Mek1/2 Kinases Are Dispensable for *K-Ras*^{G12V}-Driven NSCLCs

We also evaluated the effect of eliminating the Mek1/2 kinases on tumor development. To this end we used *Mek1*$^{lox/lox}$ (Catalanotti et al., 2009) and *Mek2*$^{-/-}$ (Belanger et al., 2003) strains since Mek1, but not Mek2, is required for survival during embryonic development (Giroux et al., 1999; Belanger et al., 2003; Bissonauth et al., 2006). Survival of Ad-Cre treated *K-Ras*$^{+/G12V}$;*Mek1*$^{lox/lox}$ mice (n = 14) was slightly increased (50% survival at 44 versus 37.5 weeks in control mice [n = 20], a 22% increase) (Figure 3A). Similar results were observed with *K-Ras*$^{+/G12V}$;*Mek2*$^{-/-}$ mice (n = 19) (50% survival at 52 versus 45 weeks in control animals [n = 20], a 19% increase) (Figure 3A). When these mice were sacrificed 6 months after exposure to Ad-Cre, they displayed a similar tumor burden as control animals carrying wild-type *Mek* alleles (Figure 3B). Southern blot analysis of individual tumors isolated from *K-Ras*$^{+/G12V}$;

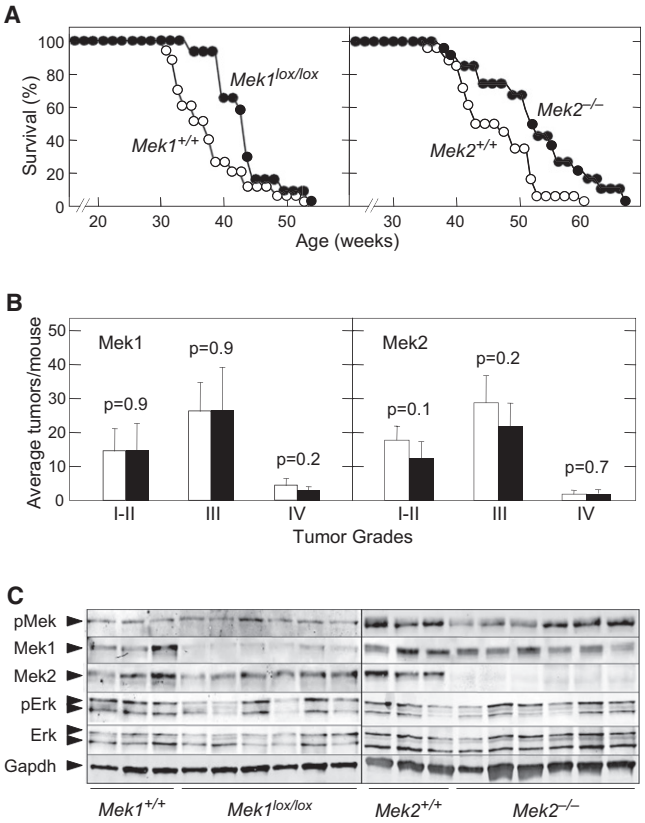

Figure 3. *K-Ras*^{G12V} Induces NSCLCs in the Absence of Mek1 or Mek2

(A) The left panel shows survival of *K-Ras*$^{+/G12V}$;*Mek1*$^{+/+}$ (n = 20) (open circles) and *K-Ras*$^{+/G12V}$;*Mek1*$^{lox/lox}$ (n = 14) (solid circles) mice treated with Ad-Cre at 8 weeks of age. The right panel illustrates survival of *K-Ras*$^{+/G12V}$;*Mek2*$^{+/+}$ (n = 20) (open circles) and *K-Ras*$^{+/G12V}$;*Mek2*$^{-/-}$ (n = 19) (solid circles) mice treated with Ad-Cre at 8 weeks of age.

(B) The left panel shows the number of tumors, classified by grade (I–IV), observed in *K-Ras*$^{+/G12V}$;*Mek1*$^{+/+}$ (n = 7) (open bars) and *K-Ras*$^{+/G12V}$;*Mek1*$^{lox/lox}$ (n = 6) (solid bars) mice sacrificed 6 months after Ad-Cre treatment. The right panel illustrates the number of tumors, classified by grade (I–IV), observed in *K-Ras*$^{+/G12V}$;*Mek2*$^{+/+}$ (n = 5) (open bars) and *K-Ras*$^{+/G12V}$;*Mek2*$^{-/-}$ (n = 5) (solid bars) mice sacrificed 6 months after Ad-Cre treatment. Error bars indicate mean ± SD. p values were calculated according to Student's t test.

(C) Western blot analysis of pMek, Mek1, Mek2, pErk1/2, and Erk1/2 expression in lysates derived from individual tumors of the indicated genotype collected 8 months after Ad-Cre treatment. Gapdh was used as loading control. Migration of the above proteins is indicated by arrowheads.

See also Figure S3.

Mek1$^{lox/lox}$ mice revealed that *Mek1*^{lox} alleles had undergone efficient recombination (Figure S3). Indeed, the levels of expression of Mek1 in these tumors were almost undetectable (Figure 3C). As expected, Mek2 could not be detected in tumors isolated from *K-Ras*$^{+/G12V}$;*Mek2*$^{-/-}$ animals (Figure 3C).

As previously observed with Erk kinases, loss of Mek1 did not result in increased Mek2 expression (Figure 3C). Likewise, the levels of Mek1 were similar in tumors derived from *Mek2*$^{-/-}$ and *Mek2*$^{+/+}$ control mice. No changes were observed in the levels of pMek proteins in those tumors generated in the absence of Mek1 or Mek2 (Figure 3C). Finally, loss of one of the two Mek kinases had no significant effect on overall Mek activity, as determined by the normal phosphorylation levels displayed by their downstream targets, Erk1/2 (Figure 3C).

Mek1/2 Kinases Are Essential for Tumor Development and Normal Homeostasis

To determine whether both Mek kinases were required for NSCLC, we exposed *K-Ras*$^{+/G12V}$;*Mek1*$^{lox/lox}$;*Mek2*$^{-/-}$ mice to Ad-Cre. These mice displayed significantly increased survival when compared with control *K-Ras*$^{+/G12V}$;*Mek1*$^{+/+}$;*Mek2*$^{+/+}$ animals. Whereas the control cohort (n = 10) had a 50% survival rate of 33 weeks, *K-Ras*$^{+/G12V}$;*Mek1*$^{lox/lox}$;*Mek2*$^{-/-}$ mice (n = 14) had a 50% survival rate at 57 weeks (Figure 4A), thus displaying an almost 100% increase in survival. As illustrated in the case of the Erk kinases, tumors present in *K-Ras*$^{+/G12V}$;*Mek1*$^{lox/lox}$;*Mek2*$^{-/-}$ mice examined 6 months after Ad-Cre treatment (n = 6) carried unrecombined *Mek1*^{lox} alleles and expressed normal levels of Mek1 (Figures 4B and 4C). These observations indicate that Mek1 expression was essential for tumor development in the absence of Mek2 (Figure 4D).

To examine whether Mek kinase activity was essential for adult homeostasis, *Mek1*$^{lox/lox}$;*Mek2*$^{-/-}$;*RERT*$^{ert/ert}$ mice were exposed to a tamoxifen diet at 30 days of age. These mice (n = 6) also displayed a rapid deterioration of their health, leading to death just 2 weeks after starting the tamoxifen diet (Figure 4E). Southern blot analysis of DNA isolated from tissues of sick/moribund animals revealed recombination rates of *Mek1*^{lox} alleles ranging from 70% to 80% in most tissues (Figure S4A). These observations indicate that the Mek kinases are also essential for adult homeostasis. Whether a single *Mek* allele might be sufficient to sustain adult life remains to be determined.

Necropsy analysis of moribund mice reveled multiple defects, including severe alterations in the structure of intestinal and colonic tissue incompatible with life (Figure S4B). Even limited ablation of *Mek* alleles resulted in significant alterations of the normal architecture, including distorted crypts, blunted and shorter villi, increased lamina propria, and goblet cell hyperplasia. Likewise, the colonic tissue of *Mek1*$^{lox/lox}$;*Mek2*$^{-/-}$;*RERT*$^{ert/ert}$ mice displayed loss as well as severe shortening of the crypts (Figure S4B).

B-Raf Is Dispensable for *K-Ras*^{G12V}-Induced NSCLCs

Raf kinases—A-Raf, B-Raf, and c-Raf—do not have full compensatory activities during embryonic and early postnatal development (Galabova-Kovacs et al., 2006). To examine whether they also played unique roles during *K-Ras*^{G12V}-driven NSCLC, we crossed *K-Ras*$^{+/G12V}$ mice with *B-Raf*$^{lox/lox}$ (Chen et al., 2006) and *c-Raf*$^{lox/lox}$ (Jesenberger et al., 2001) animals and submitted them to infection with Ad-Cre particles. As illustrated in Figure 5A, conditional ablation of *B-Raf*^{lox} alleles in *K-Ras*^{G12V}-induced NSCLC did not increase survival (50% survival of *K-Ras*$^{+/G12V}$;*B-Raf*$^{lox/lox}$ mice [n = 25] at 41.5 versus 40 weeks in *K-Ras*$^{+/G12V}$;*B-Raf*$^{+/+}$ control animals [n = 28], a 5% increase). The number and grade of tumors in mice lacking B-Raf 6 months after Ad-Cre treatment were similar to those present in control mice (Figures 5B and 5C). Efficient recombination of the *B-Raf*^{lox} alleles in tumor tissue was determined by Southern (Figure S5) and western (Figure 5D) blot analysis. Immunohistochemistry staining with an anti-B-Raf antibody

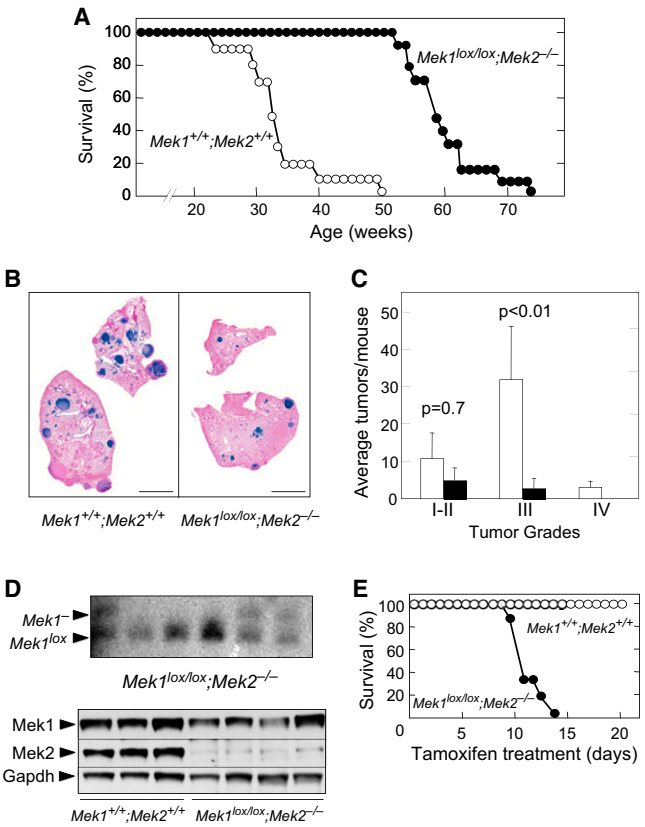

Figure 4. Elimination of Mek1/2 Kinases Prevents Induction of NSCLCs by an Endogenous *K-Ras*^{G12V} Oncogene

(A) Survival of *K-Ras*$^{+/G12V}$;*Mek1*$^{+/+}$;*Mek2*$^{+/+}$ (n = 10) (open circles) and *K-Ras*$^{+/G12V}$;*Mek1*$^{lox/lox}$;*Mek2*$^{-/-}$ (n = 14) (solid circles) mice treated with Ad-Cre at 8 weeks of age.

(B) Whole-mount X-Gal staining of lung sections collected from mice with the indicated genotypes 6 months after Ad-Cre treatment. β-Geo positive cells identified by X-Gal staining (blue color) correspond to cells expressing K-Ras^{G12V}. Scale bars, 5 mm.

(C) Number of tumors, classified by grade (I–IV), observed in *K-Ras*$^{+/G12V}$;*Mek1*$^{+/+}$;*Mek2*$^{+/+}$ (n = 6) (open bars) and *K-Ras*$^{+/G12V}$;*Mek1*$^{lox/lox}$;*Mek2*$^{-/-}$ (n = 8) (solid bars) mice. Error bars indicate mean ± SD. p values were calculated according to Student's t test.

(D) The top panel shows Southern blot analysis of genomic DNA isolated from individual tumors of *K-Ras*$^{+/G12V}$;*Mek1*$^{lox/lox}$;*Mek2*$^{-/-}$ mice 8 months after Ad-Cre treatment. DNAs were digested with HindIII and probed with a 680 bp DNA fragment obtained from a region downstream from the second loxP site. The migration of the unrecombined *Mek1*^{lox} allele (1.7 kbp) and the *Mek1*$^{-}$ allele (1.5 kbp) is indicated by arrowheads. The bottom panel shows western blot analysis of Mek1 and Mek2 expression in lysates obtained from individual tumors collected 8 months after Ad-Cre treatment of *K-Ras*$^{+/G12V}$;*Mek1*$^{+/+}$;*Mek2*$^{+/+}$ and *K-Ras*$^{+/G12V}$;*Mek1*$^{lox/lox}$;*Mek2*$^{-/-}$ mice. The presence of Mek1 in tumors of Ad-Cre treated *K-Ras*$^{+/G12V}$;*Mek1*$^{lox/lox}$;*Mek2*$^{-/-}$ mice, due to partial cleavage of the *Mek1*^{lox} allele, indicates that Mek1 is essential for tumor development. Gapdh was used as loading control. Migration of the above proteins is indicated by arrowheads.

(E) Survival of *Mek1*$^{+/+}$;*Mek2*$^{+/+}$;*RERT*$^{ert/ert}$ (n = 6) (open circles) and *Mek1*$^{lox/lox}$;*Mek2*$^{-/-}$;*RERT*$^{ert/ert}$ (n = 6) (solid circles) mice fed ad libitum a tamoxifen-containing diet to activate the knocked in CreERT2 recombinase encoded by the *RERT*^{ert} alleles.

See also Figure S4.

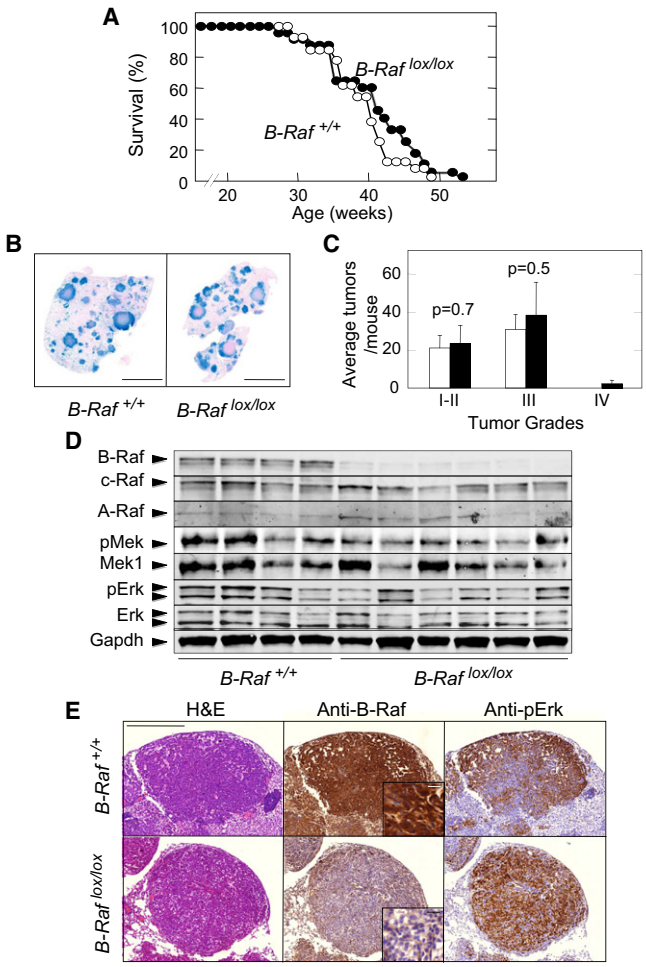

Figure 5. B-Raf Is Not Required for *K-Ras*$^{+/G12V}$-Induced NSCLCs in Mice

(A) Survival of *K-Ras*$^{+/G12V}$;*B-Raf*$^{+/+}$ (n = 28) (open circles) and *K-Ras*$^{+/G12V}$;*B-Raf*$^{lox/lox}$ (n = 25) (solid circles) mice treated with Ad-Cre at 8 weeks of age.

(B) Whole-mount X-Gal staining of lung sections collected from mice with the indicated genotypes 6 months after Ad-Cre treatment. β-Geo positive cells identified by X-Gal staining (blue color) correspond to cells expressing K-Ras^{G12V}. Scale bars, 5 mm.

(C) Number of tumors, classified by grade (I–IV), observed in *K-Ras*$^{+/G12V}$;*B-Raf*$^{+/+}$ (n = 5) (open bars) and *K-Ras*$^{+/G12V}$;*B-Raf*$^{lox/lox}$ (n = 5) (solid bars) mice. Error bars indicate mean ± SD. p values were calculated according to Student's t test.

(D) Western blot analysis of B-Raf, c-Raf, A-Raf, pMek, Mek1, pErk1/2, and Erk1/2 expression in lysates derived from individual tumors of the indicated genotype collected 8 months after Ad-Cre treatment. Gapdh was used as loading control. Migration of the above proteins is indicated by arrowheads.

(E) Tumors retained phosphorylated Erk expression in the absence of B-Raf. Hematoxylin and eosin (H&E) (left panels) and immunohistochemical staining of consecutive paraffin-fixed sections using anti-B-Raf (center panels) and anti-pErk (right panels) antibodies. Sections were obtained from lungs of Ad-Cre treated *K-Ras*$^{+/G12V}$;*B-Raf*$^{+/+}$ (top panels) and *K-Ras*$^{+/G12V}$;*B-Raf*$^{lox/lox}$ (bottom panels) mice. Insets show detail of larger areas. Scale bars, 0.5 mm (main field) and 0.02 mm (inset).

See also Figure S5.

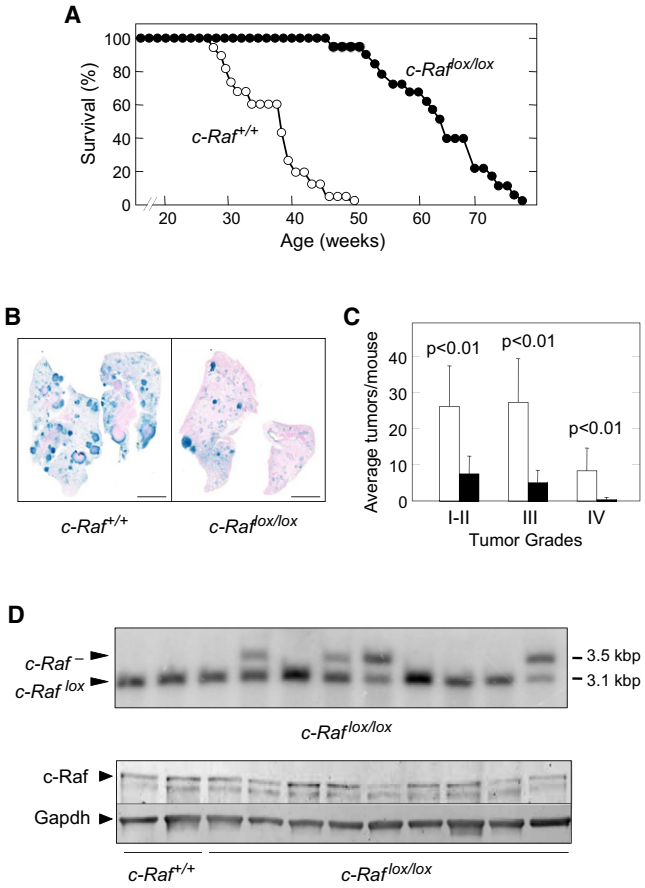

Figure 6. c-Raf Is Essential for *K-Ras*$^{+/G12V}$-Induced NSCLCs in Mice

(A) Survival of *K-Ras*$^{+/G12V}$;*c-Raf*$^{+/+}$ (n = 22) (open circles) and *K-Ras*$^{+/G12V}$;*c-Raf*$^{lox/lox}$ (n = 23) (solid circles) mice treated with Ad-Cre at 8 weeks of age.

(B) Whole-mount X-Gal staining of lung sections collected from mice with the indicated genotypes 6 months after Ad-Cre treatment. β-Geo positive cells identified by X-Gal staining (blue color) correspond to cells expressing K-Ras^{G12V}. Scale bars, 5 mm.

(C) Number of tumors, classified by grade (I–IV), observed in *K-Ras*$^{+/G12V}$;*c-Raf*$^{+/+}$ (n = 8) (open bars) and *K-Ras*$^{+/G12V}$;*c-Raf*$^{lox/lox}$ (n = 8) (solid bars) mice. Error bars indicate mean ± SD. p values were calculated according to Student's t test.

(D) The top panel shows Southern blot analysis of DNA isolated from individual tumors obtained from *K-Ras*$^{+/G12V}$;*c-Raf*$^{lox/lox}$ mice infected with Ad-Cre particles at 8 weeks of age. Tumor DNAs were digested with PstI. The sizes of the diagnostic DNA fragments for *c-Raf*^{lox} and *c-Raf*$^{-}$ alleles are indicated. The bottom panel illustrates western blot analysis of c-Raf expression in lysates obtained from individual tumors collected 8 months after Ad-Cre treatment of *K-Ras*$^{+/G12V}$;*c-Raf*$^{+/+}$ and *K-Ras*$^{+/G12V}$;*c-Raf*$^{lox/lox}$ mice. The presence of c-Raf in tumors of Ad-Cre treated *K-Ras*$^{+/G12V}$;*c-Raf*$^{lox/lox}$ mice is due to incomplete cleavage of the *c-Raf*^{lox} allele. These results indicate that c-Raf is essential for tumor development. Gapdh was used as loading control. Migration of the above proteins is indicated by arrowheads.

See also Figure S6.

further confirmed the absence of B-Raf expression in tumor tissue (Figure 5E). Interestingly, elimination of B-Raf expression had no effect on the levels of Mek and Erk phosphorylation, as determined by either western blot (Figure 5D) or immunohistochemical (Figure 5E) analysis. These observations suggest that in the absence of B-Raf, other Raf proteins can maintain mitogenic signaling through the Mek/Erk pathway. This compensatory effect did not involve increased expression of the other Raf kinases (Figure 5D).

c-Raf Is Essential to Mediate Oncogenic Signaling in *K-Ras*^{G12V}-Driven NSCLCs

Next, we investigated whether c-Raf kinase was also dispensable for *K-Ras*^{G12V}-driven NSCLCs. Ad-Cre treated *K-Ras*$^{+/G12V}$;*c-Raf*$^{lox/lox}$ mice survived significantly longer than the control cohort. Whereas 50% of *K-Ras*$^{+/G12V}$;*c-Raf*$^{+/+}$ animals (n = 22) had to be sacrificed by 38 weeks of age, half of *K-Ras*$^{+/G12V}$;*c-Raf*$^{lox/lox}$ mice (n = 23) were alive at 63 weeks. This difference represents an 83% increase in survival (Figure 6A). As expected, this increased survival was a direct consequence of the reduced number of tumors present in *K-Ras*$^{+/G12V}$;*c-Raf*$^{lox/lox}$ mice 6 months after Ad-Cre treatment (Figures 6B and 6C). More importantly, each tumor tested (n = 11) retained *c-Raf*^{lox} alleles (Figure 6D). These results were confirmed by western blot analysis of nine independent tumors (Figure 6D). These observations indicate that NSCLCs driven by K-Ras^{G12V} cannot develop in the absence of c-Raf and that the tumors responsible for the death of the *K-Ras*$^{+/G12V}$;*c-Raf*$^{lox/lox}$ mice must be "escapers," as previously observed in mice lacking Erk1/2 and Mek1/2 kinases.

Systemic Depletion of c-Raf and B-Raf Kinases in Adult Mice Is Well Tolerated

To ascertain whether c-Raf expression was required for adult tissues, we fed 30-day-old *c-Raf*$^{lox/lox}$;*RERT*$^{ert/ert}$ mice a tamoxifen diet for 3 months. Unlike mice deprived of Erk or Mek expression, *c-Raf*$^{lox/lox}$;*RERT*$^{ert/ert}$ mice did not show loss of body weight or decreased activity during this period of time. None of the tissues obtained from mice sacrificed at the end of the dietary treatment displayed obvious anatomical defects (data not shown) despite efficient recombination of *c-Raf*^{lox} alleles in most organs (60%–100% excision) (Figure 7A). Brain tissue served as a negative control because tamoxifen crosses the blood-brain barrier rather inefficiently.

Available Raf kinase inhibitors display limited selectivity (Tsai et al., 2008), suggesting that they may result in systemic inhibition of all Raf kinases. Because A-Raf conditional mutant mice are not available, we investigated whether concomitant ablation of *B-Raf* and *c-Raf* loci in adult mice had deleterious consequences. *B-Raf*$^{lox/lox}$;*c-Raf*$^{lox/lox}$;*RERT*$^{ert/ert}$ mice exposed to a tamoxifen diet for 3 months remained healthy and did not show weight loss or behavioral changes. Moreover, histological examination of 20 different tissues at the end of the treatment did not reveal detectable abnormalities (data not shown). These tissues displayed efficient recombination of the *B-Raf*^{lox} and/or *c-Raf*^{lox} alleles, ranging from 80% to 100% excision in the case of *B-Raf*^{lox} and 60% to 100% in the case of *c-Raf*^{lox} (Figure 7B). Brain tissue served as a negative control.

Analysis of these tissues for the expression of A-Raf indicated that this isoform is widely expressed, even in the absence of *B-Raf* and *c-Raf* alleles, thus suggesting that A-Raf may compensate for the absence of the other Raf isoforms (Figure S6). Interestingly, the levels of pMek and pErk showed significant variation from tissue to tissue. Yet, within a given tissue, we did not observe significant variation in the levels of Mek and Erk phosphorylation, regardless of the extent to which the *B-Raf* and

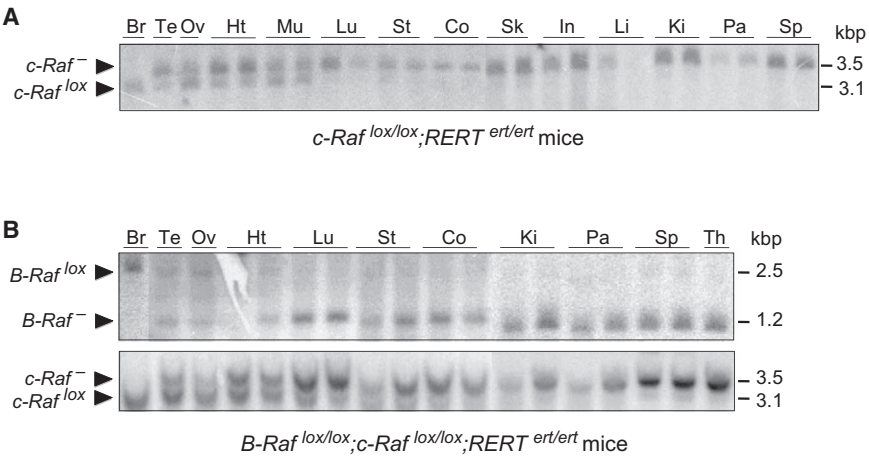

Figure 7. Adult Mice Tolerate Widespread Ablation of *B-Raf* and *c-Raf* Alleles

(A) Southern blot analysis of DNA isolated from tissues of *c-Raf*$^{lox/lox}$;*RERT*$^{ert/ert}$ mice fed ad libitum with a tamoxifen diet for 3 months (P30–P120). DNA was digested with PstI and probed with a 854 bp DNA fragment corresponding to sequences located in intron 4 downstream from the second loxP site. Migration of the ablated *c-Raf*$^{-}$ allele and the unrecombined *c-Raf*^{lox} allele is indicated by arrowheads. The sizes of the diagnostic DNA fragments for these alleles are also indicated. Whereas some tissues such as testis (Te), ovaries (Ov), heart (Ht), and muscle (Mu) display partial *c-Raf*^{lox} cleavage (from 50% to 70%), the majority of the tissues, including lung (Lu), stomach (St), colon (Co), skin (Sk), intestine (In), liver (Li), kidney (Ki), pancreas (Pa), and spleen (Sp), showed complete or almost complete excision. Brain tissue (Br) served as negative control because tamoxifen crosses the brain-blood barrier with limited efficiency.

(B) Southern blot analysis of DNA isolated from tissues of *B-Raf*$^{lox/lox}$;*c-Raf*$^{lox/lox}$;*RERT*$^{ert/ert}$ mice fed ad libitum with a tamoxifen diet for 3 months (P30–P120). DNA samples were digested with HindIII and probed with a 422 bp DNA fragment corresponding to sequences located in intron 12 upstream from the first loxP site. Migration of the ablated *B-Raf null* (*B-Raf*$^{-}$) and *c-Raf null* (*c-Raf*$^{-}$) alleles as well as of the unrecombined *B-Raf*^{lox} and *c-Raf*^{lox} alleles is indicated by arrowheads. The sizes of the diagnostic DNA fragments for these alleles are also indicated. The top panel shows *B-Raf*^{lox} alleles that are almost completely recombined in lung (Lu), stomach (St), colon (Co), kidney (Ki), pancreas (Pa), spleen (Sp), and thymus (Th) and only partially cleaved in testis (Te), ovaries (Ov), and heart (Ht). The bottom panel illustrates *c-Raf*^{lox} alleles that were partially excised in testis (Te), ovaries (Ov), heart (Ht), lung (Lu), stomach (St), and colon (Co) and completely recombined in kidney (Ki), pancreas (Pa), spleen (Sp), and thymus (Th). Brain tissue (Br) served as negative control.

See also Figure S7.

c-Raf alleles had been ablated (Figure S6). These observations may explain the lack of defects observed in adult *B-Raf*$^{lox/lox}$;*c-Raf*$^{lox/lox}$;*RERT*$^{ert/ert}$ mice.

c-Raf Blocks *K-Ras* Oncogene Signaling in NSCLCs by a Mechanism Other than Inducing Senescence or Apoptosis

Next, we examined the mechanisms by which ablation of c-*Raf* impaired tumor development in response to K-Ras^{G12V} signaling. Expression of *K-Ras*^{G12V} in lung cells lacking Cdk4 induces an immediate senescence response that prevents cell proliferation (Puyol et al., 2010). However, lung sections of *K-Ras*$^{+/G12V}$;*c-Raf*$^{lox/lox}$ mice did not display detectable senescent cells 4 weeks after turning on *K-Ras*^{G12V} expression, as determined by the absence of senescence-associated β-galactosidase (SA-β-gal) staining (Figure S7A). Similar results were obtained at an earlier time point of 2 weeks (data not shown). As a positive control, sections from *K-Ras*$^{+/G12V}$;*Cdk4*$^{-/-}$ animals displayed SA-β-gal positive cells (Figure S7A).

It has been described that c-Raf protects cells from apoptosis (Mikula et al., 2001; Yamaguchi et al., 2004; Piazzolla et al., 2005; Matallanas et al., 2007). Thus, we reasoned that in the absence of c-Raf, K-Ras^{G12V} expression might lead to rapid apoptotic death of lung cells. However, lung sections of *K-Ras*$^{+/G12V}$;*c-Raf*$^{lox/lox}$ mice taken 4 weeks after turning on K-Ras^{G12V} expression did not display detectable levels of active Caspase 3 (Figure S7B). Similar results were obtained at earlier time points (data not shown). These observations indicate that ablation of c-Raf expression did not result in increased apoptosis.

We have also examined the fate of K-Ras^{G12V} expressing cells upon ablation of *c-Raf*^{lox} alleles. To this end we took advantage of the expression of β-Geo as a surrogate marker for the K-Ras^{G12V} oncoprotein (Guerra et al., 2003). In this experiment, Cre recombinase activity was provided by the *RERT*$^{ert/ert}$ alleles instead of Ad-Cre to avoid inducing an inflammatory response that may interfere with detection of β-Geo expression. As illustrated in Figure S7C, *K-Ras*$^{+/G12V}$;*c-Raf*$^{+/+}$;*RERT*$^{ert/ert}$ and *K-Ras*$^{+/G12V}$;*c-Raf*$^{lox/lox}$;*RERT*$^{ert/ert}$ mice displayed the same number of K-Ras^{G12V} positive cells (based on the surrogate β-Geo expression) 15 days after 4OHT exposure, suggesting that loss of c-Raf expression did not induce death of K-Ras^{G12V}-containing lung cells. Moreover, the number of K-Ras^{G12V} positive cells remained constant 2 weeks later despite lacking c-Raf. These observations suggest that elimination of c-Raf does not result in death of K-Ras^{G12V}-expressing lung cells.

We have recently shown that ablation of *c-Raf* in skin tumors driven by constitutive activation of the Ras-GEF, SOS, resulted in tumor disappearance due to increased terminal differentiation of tumor cells (Ehrenreiter et al., 2009). These effects were mediated by the synchronous activation of the Rok kinase upon *c-Raf* ablation (Ehrenreiter et al., 2009). Unfortunately, more than 30% of lung cells, regardless of genotype, had an active Rok kinase, as determined by the presence of phosphorylated Cofilin, a downstream target of this kinase (data not shown). Thus, it was not possible to determine whether the lack of proliferation of lung cells deprived of c-Raf was mediated by Rok activation.

K-Ras Signals through B-Raf and c-Raf in Mouse Embryonic Fibroblasts and in Human NSCLC Cell Lines

We have also explored whether the requirement of c-Raf for K-Ras^{G12V} signaling was cell type dependent. Cultures of primary MEFs from E13.5 *K-Ras*$^{+/G12V}$;*RERT*$^{ert/ert}$ embryos carrying *B-Raf*^{lox} and *c-Raf*^{lox} alleles, either individually or in combination (n = 3), were exposed to 4OHT for 5 days to activate the resident CreERT2 recombinase to induce K-Ras^{G12V}

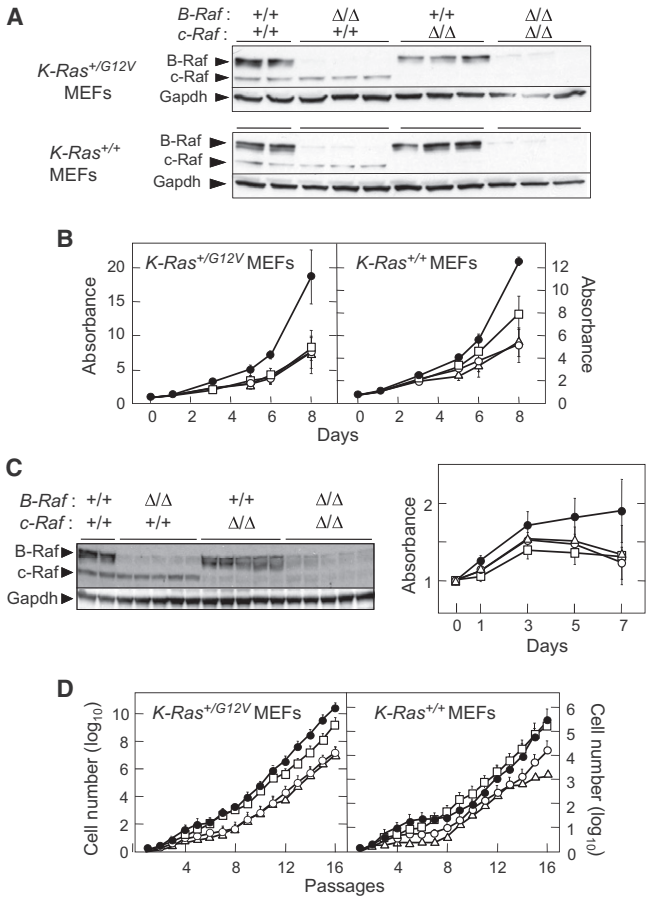

Figure 8. B-Raf and c-Raf Are Not Essential for Proliferation and Immortalization of Primary MEFs Driven by Wild-Type or Oncogenic K-Ras Signaling

(A) Western blot analysis of B-Raf and c-Raf protein expression in primary MEFs derived from (top panel) three independent *K-Ras*$^{+/G12V}$;*RERT*$^{ert/ert}$, *K-Ras*$^{+/G12V}$;*B-Raf*$^{lox/lox}$;*RERT*$^{ert/ert}$, *K-Ras*$^{+/G12V}$;*c-Raf*$^{lox/lox}$;*RERT*$^{ert/ert}$, and *K-Ras*$^{+/G12V}$;*B-Raf*$^{lox/lox}$;*c-Raf*$^{lox/lox}$;*RERT*$^{ert/ert}$ embryos, and (bottom panel) three independent *K-Ras*$^{+/+}$;*RERT*$^{ert/ert}$, *K-Ras*$^{+/+}$;*B-Raf*$^{lox/lox}$;*RERT*$^{ert/ert}$, *K-Ras*$^{+/+}$;*c-Raf*$^{lox/lox}$;*RERT*$^{ert/ert}$, and *K-Ras*$^{+/+}$;*B-Raf*$^{lox/lox}$;*c-Raf*$^{lox/lox}$;*RERT*$^{ert/ert}$ embryos. These MEFs were incubated in DMEM supplemented with 10% FBS in the presence of 4OHT for 5 days to activate expression of the resident *K-Ras*$^{+/G12V}$ oncogene and to eliminate the *c-Raf*^{lox} (*c-Raf*^{Δ}) and/or *B-Raf*^{lox} (*B-Raf*^{Δ}) conditional alleles. Gapdh served as loading control. Migration of the corresponding proteins is indicated by arrowheads.

(B) Growth curves of the primary MEFs (n = 3) described above. MEFs were grown in DMEM supplemented with 10% FBS and 600 nM 4OHT for 5 days before seeding. Results are shown in arbitrary absorbance units. Left panel shows *K-Ras*$^{+/G12V}$;*RERT*$^{ert/ert}$ (solid circles), *K-Ras*$^{+/G12V}$;*B-Raf*$^{Δ/Δ}$;*RERT*$^{ert/ert}$ (open squares), *K-Ras*$^{+/G12V}$;*c-Raf*$^{Δ/Δ}$;*RERT*$^{ert/ert}$ (open circles), and *K-Ras*$^{+/G12V}$;*B-Raf*$^{Δ/Δ}$;*c-Raf*$^{Δ/Δ}$;*RERT*$^{ert/ert}$ (open triangles). Right panel illustrates *K-Ras*$^{+/+}$;*RERT*$^{ert/ert}$ (solid circles), *K-Ras*$^{+/+}$;*B-Raf*$^{Δ/Δ}$;*RERT*$^{ert/ert}$ (open squares), *K-Ras*$^{+/+}$;*c-Raf*$^{Δ/Δ}$;*RERT*$^{ert/ert}$ (open circles), and *K-Ras*$^{+/+}$;*B-Raf*$^{Δ/Δ}$;*c-Raf*$^{Δ/Δ}$;*RERT*$^{ert/ert}$ (open triangles). Error bars indicate mean ± SD.

(C) The left panel shows western blot analysis of B-Raf and c-Raf protein expression in primary MEFs derived from five independent *K-Ras*$^{+/G12V}$;*B-Raf*$^{lox/lox}$;*RERT*$^{ert/ert}$, *K-Ras*$^{+/G12V}$;*c-Raf*$^{lox/lox}$;*RERT*$^{ert/ert}$, and *K-Ras*$^{+/G12V}$;*B-Raf*$^{lox/lox}$;*c-Raf*$^{lox/lox}$;*RERT*$^{ert/ert}$ embryos. Samples from two *K-Ras*$^{+/G12V}$;*RERT*$^{ert/ert}$ embryos are also shown. MEFs were incubated in DMEM supplemented with 2% FBS in the presence of 4OHT for 5 days to activate expression of the resident *K-Ras*^{G12V} oncogene and to eliminate the *c-Raf*^{lox} (*c-Raf*^{Δ}) and/or *B-Raf*^{lox} (*B-Raf*^{Δ}) conditional alleles. Gapdh served as loading control. Migration of the corresponding proteins is indicated by arrowheads. The right panel shows growth curves of the primary MEFs (n = 5) described above. MEFs were grown in DMEM supplemented with 2% FBS and 600 nM 4OHT. *K-Ras*$^{+/G12V}$;*RERT*$^{ert/ert}$ (solid circles), *K-Ras*$^{+/G12V}$;*B-Raf*$^{Δ/Δ}$;*RERT*$^{ert/ert}$ (open squares), *K-Ras*$^{+/G12V}$;*c-Raf*$^{Δ/Δ}$;*RERT*$^{ert/ert}$ (open circles), and *K-Ras*$^{+/G12V}$;*B-Raf*$^{Δ/Δ}$;*c-Raf*$^{Δ/Δ}$;*RERT*$^{ert/ert}$ (open triangles). Error bars indicate mean ± SD.

(D) Immortalization of the primary MEFs described in (B) following a 3T3 protocol (n = 3). Cells were cultivated in DMEM supplemented with 10% FBS and 600 nM 4OHT. Symbols are those described in (B). Error bars indicate mean ± SD.

See also Figure S8.

expression and to ablate the conditional *B-Raf* and *c-Raf* alleles (Figure 8A). Inhibition of c-Raf expression partially decreased but did not eliminate proliferation of K-Ras^{G12V}-expressing primary MEFs (Figure 8B). Similar results were obtained when we inhibited B-Raf expression. Moreover, concomitant inhibition of both proteins did not result in synergistic or additive effects (Figure 8B). Similar results were obtained using limiting serum conditions (2% fetal bovine serum [FBS]) (Figure 8C). The partial requirement of B-Raf and c-Raf expression for proper proliferation was not unique to MEFs expressing K-Ras oncogenes. In agreement with previous observations, wild-type MEFs also required c-Raf for optimal proliferation (Mikula et al., 2001). Elimination of c-Raf and B-Raf, either alone or in combination, also resulted in partial inhibition of their proliferative properties (Figure 8B).

We also examined whether B-Raf and c-Raf kinases were required for immortalization of primary MEFs (Guerra et al., 2003; Tuveson et al., 2004). Inhibition of B-Raf had little, if any, effect on the immortalization rate of K-Ras^{G12V}-expressing MEFs and did not induce proliferative senescence. Inhibition of c-Raf, either alone or in combination with B-Raf, did not affect the immortalization rate (Figure 8D). MEFs expressing wild-type K-Ras underwent the expected proliferative senescence. This process was exacerbated by inhibition of c-Raf, but not of B-Raf (Figure 8D). However, these MEFs became immortal after a few passages regardless of whether they lacked c-Raf alone or c-Raf plus B-Raf. These results indicate that neither B-Raf nor c-Raf proteins are essential for proliferation or immortalization of MEFs, regardless of whether they expressed normal or oncogenic K-Ras proteins.

Finally, we examined the effect of knocking down c-RAF and B-RAF expression in human NSCLC cell lines containing *K-RAS* oncogenes. To this end we selected four cell lines, A549, H23, H358, and H441, of which only the last two have shown a strong dependency ("addiction") on *K-RAS* oncogenes (Singh et al., 2009). As illustrated in Figure S8, the extent of ERK phosphorylation was not significantly affected by knock down of c-RAF or B-RAF expression. However, inhibition of c-RAF or B-RAF affected their proliferation rate, although this inhibition appeared to be unrelated to the relative addiction of these cell lines to *K-RAS* oncogene expression. Moreover, as illustrated above for MEFs, knock down of c-RAF and B-RAF had a similar inhibitory effect on the proliferation rate of each of the respective NSCLC cell lines (Figure S8). These observations indicate that the exquisite requirement for c-Raf expression observed in the K-Ras^{G12V}-driven NSCLC tumor model reported here might not be a general property of K-Ras signaling. Alternatively, inhibition of c-Raf and B-Raf expression may have different consequences under in vitro growth conditions.

DISCUSSION

K-RAS oncogenes signal through a cascade of downstream effectors, most of which are druggable kinases. Yet, to our knowledge, there are no approved targeted therapies to treat *K-RAS*-driven NSCLC. This situation may stem from our limited knowledge of what effectors are directly responsible for mediating K-RAS signaling in this tumor type and, hence, serve as effective therapeutic targets. As illustrated in this study, each one of the two Erk kinases, Erk1 or Erk2, is sufficient to allow initiation of *K-Ras*-induced NSCLC. However, K-Ras oncogenes could not transform lung cells in the absence of both Erk kinases. Unfortunately, widespread loss of the Erk1/2 kinases resulted in severe toxicity that led to the rapid death of the animal even when only a limited percentage of cells (ranging from 40% to 60% depending on the tissue type) lost both Erk kinases. Yet, a single *Erk* allele was sufficient to sustain normal adult homeostasis. Hence, limited inhibition of ERK kinase activity within a tolerated therapeutic window may provide a successful pharmacological approach to treat K-RAS-positive NSCLC.

Similar results were observed when we targeted the Mek kinases. Both Mek1 and Mek2 efficiently sustained *K-Ras* oncogenic signaling in the absence of the other isoform. These results differed from those observed with DMBA-induced skin tumors in which Mek2 could not compensate for the absence of Mek1 (Scholl et al., 2009), further illustrating that the contribution of individual members of the Ras/Mek/Erk pathway is likely to be cell type dependent. Moreover, complete loss of Mek kinases prevented *K-Ras*-driven NSCLC development. Unfortunately, as discussed above for their downstream Erk kinases, widespread loss of Mek1/2 kinases was incompatible with life. Dual MEK1/2 inhibitors have already been tested in early-phase clinical trials. Early inhibitors including CI-1040, AZD6244, and PD0325901 showed no significant antitumor activity at the permissible doses in a series of solid tumors, including advanced NSCLCs (Rinehart et al., 2004; Hainsworth et al., 2010; Haura et al., 2010). Recently, a more potent MEK inhibitor, GSK1120212, active on B-RAF-driven human melanoma cell lines (Villanueva et al., 2010), has yielded 2 partial responses and 9 disease stabilizations in 14 patients suffering from *K-Ras* oncogene-positive NSCLC (http://www.esmo.org/events/milan-2010-congress). These results suggest that MEK inhibition may yield therapeutic benefit to patients with NSCLC.

The immediate Ras downstream effectors within the Raf/Mek/Erk pathway are the Raf kinases, A-Raf, B-Raf, and c-Raf. B-Raf was completely dispensable for K-Ras oncogenic signaling, at least within the context of NSCLC. Moreover, phosphorylation of Erk proteins within the tumor appeared to be unaffected, suggesting that other Raf kinases mediate K-Ras oncogenic signaling in the absence of B-Raf. However, in this case the compensatory effects of c-Raf (and/or A-Raf) on B-Raf were not reciprocal. Elimination of c-Raf from *K-Ras*^{G12V}-expressing lung cells completely inhibited tumor development. Thus, neither B-Raf nor A-Raf could compensate for the lack of c-Raf. Because K-Ras is the Ras isoform that binds and activates c-Raf more efficiently (Voice et al., 1999), it is possible that c-Raf might be essential to mediate K-Ras signaling to the Mek and Erk kinases, at least in an oncogenic setting. Indeed, oncogenic RAS exclusively signaled via c-RAF to the ERK-MAPK pathway in human melanoma cell lines (Dumaz et al., 2006). However, it is also possible that c-Raf, but not B-Raf or A-Raf, may modulate an alternative downstream pathway essential for malignant transformation (Takezawa et al., 2009), but not for normal homeostasis. This hypothesis may also help to explain why elimination of c-Raf is not deleterious for adult mice.

The existence of c-Raf-dependent, Mek-independent pathways in *K-Ras* oncogene-induced tumors has been invoked before (Haigis et al., 2008). More recently, such a pathway has been shown to be essential for the development and maintenance of Ras-driven epidermal tumors (Ehrenreiter et al., 2009). In particular, loss of c-Raf in established tumors expressing a membrane-tagged SOS exchange factor induced a massive increase in terminal differentiation of the tumor cells accompanied by a sharp decline in cell proliferation, two events that resulted in tumor regression. Terminal differentiation of these SOS-expressing keratinocytes in the absence of c-Raf was mediated by activation of the Rok pathway (Ehrenreiter et al., 2009), a pathway that is normally inhibited by c-Raf via direct interaction with Rok (Niault et al., 2009). Unfortunately, the limited number of K-Ras^{G12V}-expressing cells and their inability to expand in the absence of c-Raf made it impossible for us to investigate the molecular events that prevent tumor development. If c-Raf mediates K-Ras^{G12V} signaling via protein-protein interaction with Rok or other substrates, therapeutic intervention will require strategies other than inhibition of c-Raf catalytic activity. Recent studies have suggested that different mutations in *K-RAS* may result in different clinical outcomes (De Roock et al., 2010). Whether these differences may result from different interactions with Ras effectors remains to be determined.

RAF inhibitors with activity against B-RAF and c-RAF kinases are potent inhibitors of tumors carrying a mutated B-RAF^{V600E} oncogene. However, these inhibitors activate the MEK-ERK pathway in tumors carrying mutant K-RAS or wild-type RAS/RAF molecules by a mechanism involving transactivation of one protomer in RAF homodimers and heterodimers (Hatzivassiliou et al., 2010; Poulikakos et al., 2010). Moreover, Heidorn et al. (2010) have illustrated that a kinase-dead B-Raf induces melanomas in the presence of an endogenous K-Ras oncogene. Finally, patients with melanoma treated with B-RAF inhibitors develop cutaneous squamous cell carcinomas at significant frequency (Bollag et al., 2010; Flaherty et al., 2010). Whether similar results will be observed with c-RAF selective inhibitors remains to be determined. Current efforts aimed at generating mice expressing an inducible kinase-dead c-Raf protein may also help to shed some light on this issue.

Recently, the use of synthetic lethal approaches with *K-Ras*-driven NSCLC mouse tumor models has allowed the identification of novel therapeutic targets, including the NF-κB pathway and Cdk4 (Meylan et al., 2009; Puyol et al., 2010). Ablation of Cdk4 expression in *K-Ras* oncogene containing lung cells elicited an immediate senescence response that prevented tumor initiation and progression (Puyol et al., 2010). Such response did not appear to be responsible for the lack of proliferation of *K-Ras* oncogene expressing cells in the absence of c-Raf. Thus, it is possible that c-Raf and Cdk4 inhibitors may inhibit proliferation of NSCLC cells by different mechanisms, thus resulting in synergistic antitumor effects.

Finally, it will be important to develop tumor models that address the effect of inhibiting these downstream effectors on tumor maintenance rather than on tumor development. Replacement of the Cre-lox strategy used in this study to activate K-Ras^{G12V} expression by the Flpe-frt recombinase system will allow temporal separation of tumor initiation and therapeutic intervention. Results derived from these studies are likely to provide more relevant information toward the development of effective targeted therapies for the treatment of *K-Ras* oncogene-driven NSCLC.

EXPERIMENTAL PROCEDURES

Mice

K-Ras$^{+/LSLG12Vgeo}$ (Guerra et al., 2003), *RERT*$^{ert/ert}$ (Guerra et al., 2003), *Erk1*$^{-/-}$ (Pagès et al., 1999), *Erk2*$^{lox/lox}$ (Fischer et al., 2005), *Mek1*$^{lox/lox}$ (Catalanotti et al., 2009), *Mek2*$^{-/-}$ (Belanger et al., 2003), *B-Raf*$^{lox/lox}$ (Chen et al., 2006), and *c-Raf*$^{lox/lox}$ (Jesenberger et al., 2001) strains have been previously described. All animal experiments were approved by the Ethical Committee of the CNIO and performed in accordance with the guidelines stated in the *International Guiding Principles for Biomedical Research Involving Animals*, developed by the Council for International Organizations of Medical Sciences (CIOMS). All strains were genotyped by Transnetyx (Cordova, TN, USA).

Adenovirus Intratracheal Infection

Eight to 10-week-old mice were treated once by intratracheal adeno-Cre instillation with 2.5 × 10^8 pfu/mouse of virus after anesthesia (i.p. injection of ketamine 75 mg/kg, xylazine 12 mg/kg) (Simpson et al., 2001).

Histopathology and Immunohistochemistry

For routine histological study, lung lobes were fixed in 10% buffered formalin (Sigma) and embedded in paraffin. For quantification and classification of tumor lesions, lung lobes were processed for whole-mount X-Gal staining to detect β-Geo, as a surrogate marker for K-Ras^{G12V} expression (Guerra et al., 2003). Stained tissues were embedded in paraffin, serially sectioned, and tumors counted and classified according to standard histopathological grading (Jackson et al., 2005). Antibodies used for immunostaining included those raised against: B-Raf (Abcam; ab33899); pErk (Cell Signaling Technology; 9101); pCofilin (Santa Cruz Biotechnology; sc-21867-R); and active Caspase3 (R&D Systems; AF835). For endogenous SA-β-gal detection, lung lobes were snap-frozen in O.C.T. (Sakura) and processed on 10 μm cryostat sections with a SA-β-gal staining kit (Cell Signaling Technology) in accordance with the manufacturer's recommendations. Counterstaining of cryostat sections was performed with nuclear fast red.

Western Blot Analysis

Thirty micrograms of protein extracts obtained from either tumor tissue or cell extracts were separated on SDS/PAGE gels (Bio-Rad), transferred to a nitrocellulose membrane, and blotted with antibodies raised against B-Raf (Santa Cruz Biotechnology; sc-5284), c-Raf (BD Biosciences; 610151), A-Raf (Abcam; ab19880), Mek1 (Santa Cruz Biotechnology; sc-219), Mek2 (BD Biosciences; 610235), pMek (Cell Signaling Technology; 9154), Erk (Santa Cruz Biotechnology; sc-93), pErk (Cell Signaling Technology; 9101), Rsk (Santa Cruz Biotechnology; sc-231), pRsk (Cell Signaling Technology; 9341), and Gapdh (Sigma; G8795). Primary antibodies were detected with goat secondary antibodies directed against mouse or rabbit IgGs (Alexa Fluor 680; Invitrogen) and visualized with Odyssey Infrared Imaging System (LI-COR Biosciences).

Cell Culture Assays

MEFs were isolated from E13.5 embryos and propagated according to standard 3T3 protocols. All experiments were carried out in the presence of 600 nM 4OHT (Sigma). For proliferation assays, MEFs were treated for 5 days with 4OHT to ablate the conditional *B-Raf*^{lox} and *c-Raf*^{lox} alleles, seeded on 96-well plates (1000 cells/well) in triplicate in DMEM supplemented with 10% FBS, and their growth rate was determined by the MTT cell proliferation kit (Roche). Human NSCLC cell lines were purchased from the ATCC. Cells were infected with MISSION shRNAs directed against B-RAF or c-RAF (Sigma). Scrambled shRNA was used as control. Cells were selected with puromycin (2 μg/ml) for 5 days before seeding. For proliferation assays cells were seeded on 96-well plates (1000 cells/well) in RPMI medium supplemented with 10% FBS and puromycin, and their growth rate was determined by the MTT cell proliferation kit.

SUPPLEMENTAL INFORMATION

Supplemental Information includes eight figures and can be found with this article online at doi:10.1016/j.ccr.2011.04.002.

ACKNOWLEDGMENTS

We thank Florian A. Karreth, David A. Tuveson (Cambridge Research Institute), Christopher Murriel, David Davis, and Leisa Johnson (Genentech, Inc.) for sharing their results with us prior to publication. The generosity of Alcino J. Silva (UCLA) (*B-Raf*$^{lox/lox}$ mice), Stephen M. Hedrick (UCSD) (*Erk2*$^{lox/lox}$ mice), and Gilles Pagès and Jacques Pouysségur (University of Nice Sophia Antipolis) (*Erk1*$^{-/-}$ strain) for making their mice available to us, is much appreciated. We also thank M. San Román and R. Villar (Experimental Oncology), M. Lamparero and I. Aragón (Animal Facility), and V. Alvarez, E. Gil, M. Gómez, P. González, and N. Matesanz (Comparative Pathology) for excellent technical assistance. Work in the laboratory of M.Bar. is supported by grants from the EU-Framework Programme (LSHG-CT-2007-037665), European Research Council (250297-RAS AHEAD), Spanish Ministry of Science and Innovation (SAF2006-11773 and CSD2007-00017), Autonomous Community of Madrid (GR/SAL/0587/2004 and S2006/BIO-0232), and *Fundación de la Mutua Madrileña del Automovil*. Work in the M.Bac. laboratory is supported by the Austrian Scientific Research Fund (SEB 021) and by a grant from the EU (GROWTHSTOP). J.C. is supported by a Canadian Institutes of Health Research grant (MOP-97801). R.B.B. is supported by a BEFI grant from the *Fondo de Investigaciones Sanitarias* and S.F. by a FEBS Long-Term Fellowship and a Sara Borrell grant from the *Instituto de Salud Carlos III*.

Received: October 6, 2010
Revised: January 27, 2011
Accepted: April 1, 2011
Published online: April 21, 2011

REFERENCES

Barbie, D.A., Tamayo, P., Boehm, J.S., Kim, S.Y., Moody, S.E., Dunn, I.F., Schinzel, A.C., Sandy, P., Meylan, E., Scholl, C., et al. (2009). Systematic RNA interference reveals that oncogenic KRAS-driven cancers require TBK1. Nature *462*, 108–112.

Belanger, L.F., Roy, S., Tremblay, M., Brott, B., Steff, A.M., Mourad, W., Hugo, P., Erikson, R., and Charron, J. (2003). Mek2 is dispensable for mouse growth and development. Mol. Cell. Biol. *23*, 4778–4787.

Bissonauth, V., Roy, S., Gravel, M., Guillemette, S., and Charron, J. (2006). Requirement for Mak2k1 (Mek1) in extra-embryonic ectoderm placentogenesis. Development *133*, 3429–3440.

Bollag, G., Hirth, P., Tsai, J., Zhang, J., Ibrahim, P.N., Cho, H., Spevak, W., Zhang, C., Zhang, Y., Habets, G., et al. (2010). Clinical efficacy of a RAF inhibitor needs broad target blockade in BRAF-mutant melanoma. Nature *467*, 596–599.

Camonis, J.H., and White, M.A. (2005). Ral GTPases: corrupting the exocyst in cancer cells. Trends Cell Biol. *15*, 327–332.

Catalanotti, F., Reyes, G., Jesenberger, V., Galabova-Kovacs, G., de Matos Simoes, R., Carugo, O., and Baccarini, M. (2009). A Mek1-Mek2 heterodimer determines the strength and duration of the Erk signal. Nat. Struct. Mol. Biol. *16*, 294–303.

Chen, A.P., Ohno, M., Giese, K.P., Kühn, R., Chen, R.L., and Silva, A.J. (2006). Forebrain-specific knockout of B-raf kinase leads to deficits in hippocampal long-term potentiation, learning, and memory. J. Neurosci. Res. *83*, 28–38.

Cully, M., You, H., Levine, A.J., and Mak, T.W. (2006). Beyond PTEN mutations: the PI3K pathway as an integrator of multiple inputs during tumorigenesis. Nat. Rev. Cancer *6*, 184–192.

De Roock, W., Jonker, D.J., Di Nicolantonio, F., Sartore-Bianchi, A., Tu, D., Siena, S., Lamba, S., Arena, S., Frattini, M., Piessevaux, H., et al. (2010). Association of KRAS p.G13D mutation with outcome in patients with chemotherapy-refractory metastatic colorectal cancer treated with cetuximab. JAMA *304*, 1812–1820.

Dumaz, N., Hayward, R., Martin, J., Ogilvie, L., Hedley, D., Curtin, J.A., Bastian, B.C., Springer, C., and Marais, R. (2006). In melanoma, RAS mutations are accompanied by switching signaling from BRAF to CRAF and disrupted cyclic AMP signaling. Cancer Res. *66*, 9483–9491.

Ehrenreiter, K., Kern, F., Velamoor, V., Meissl, K., Galabova-Kovacs, G., Sibilia, M., and Baccarini, M. (2009). Raf-1 addiction in ras-induced skin carcinogenesis. Cancer Cell *16*, 149–160.

Engelman, J.A., Luo, J., and Cantley, L.C. (2006). The evolution of phosphatidylinositol 3-kinases as regulators of growth and metabolism. Nat. Rev. Genet. *7*, 606–619.

Engelman, J.A., Chen, L., Tan, X., Crosby, K., Guimaraes, A.R., Upadhyay, R., Maira, M., McNamara, K., Perera, S.A., Song, Y., et al. (2008). Effective use of PI3K and MEK inhibitors to treat mutant Kras G12D and PIK3CA H1047R murine lung cancers. Nat. Med. *14*, 1351–1356.

Fischer, A.M., Katayama, C.D., Pagès, G., Pouysségur, J., and Hedrick, S.M. (2005). The role of erk1 and erk2 in multiple stages of T cell development. Immunity *23*, 431–443.

Flaherty, K.T., Puzanov, I., Kim, K.B., Ribas, A., McArthur, G.A., Sosman, J.A., O'Dwyer, P.J., Lee, R.J., Grippo, J.F., Nolop, K., and Chapman, P.B. (2010). Inhibition of mutated, activated BRAF in metastatic melanoma. N. Engl. J. Med. *363*, 809–819.

Galabova-Kovacs, G., Kolbus, A., Matzen, D., Meissl, K., Piazzolla, D., Rubiolo, C., Steinitz, K., and Baccarini, M. (2006). ERK and beyond: insights from B-Raf and Raf-1 conditional knockouts. Cell Cycle *5*, 1514–1518.

Giroux, S., Tremblay, M., Bernard, D., Cardin-Girard, J.F., Aubry, S., Larouche, L., Rousseau, S., Huot, J., Landry, J., Jeannotte, L., et al. (1999). Embryonic death of Mek1-deficient mice reveals a role for this kinase in angiogenesis in the labyrinthine region of the placenta. Curr. Biol. *9*, 369–372.

Guerra, C., Mijimolle, N., Dhawahir, A., Dubus, P., Barradas, M., Serrano, M., Campuzano, V., and Barbacid, M. (2003). Tumor induction by an endogenous K-ras oncogene is highly dependent on cellular context. Cancer Cell *4*, 111–120.

Gupta, S., Ramjaun, A.R., Haiko, P., Wang, Y., Warne, P.H., Nicke, B., Nye, E., Stamp, G., Alitalo, K., and Downward, J. (2007). Binding of ras to phosphoinositide 3-kinase p110alpha is required for ras-driven tumorigenesis in mice. Cell *129*, 957–968.

Haigis, K.M., Kendall, K.R., Wang, Y., Cheung, A., Haigis, M.C., Glickman, J.N., Niwa-Kawakita, M., Sweet-Cordero, A., Sebolt-Leopold, J., Shannon, K.M., et al. (2008). Differential effects of oncogenic K-Ras and N-Ras on proliferation, differentiation and tumor progression in the colon. Nat. Genet. *40*, 600–608.

Hainsworth, J.D., Cebotaru, C.L., Kanarev, V., Ciuleanu, T.E., Damyanov, D., Stella, P., Ganchev, H., Pover, G., Morris, C., and Tzekova, V. (2010). A phase II, open-label, randomized study to assess the efficacy and safety of AZD6244 (ARRY-142886) versus pemetrexed in patients with non-small cell lung cancer who have failed one or two prior chemotherapeutic regimens. J. Thorac. Oncol. *5*, 1630–1636.

Hatzivassiliou, G., Song, K., Yen, I., Brandhuber, B.J., Anderson, D.J., Alvarado, R., Ludlam, M.J., Stokoe, D., Gloor, S.L., Vigers, G., et al. (2010). RAF inhibitors prime wild-type RAF to activate the MAPK pathway and enhance growth. Nature *464*, 431–435.

Haura, E.B., Ricart, A.D., Larson, T.G., Stella, P.J., Bazhenova, L., Miller, V.A., Cohen, R.B., Eisenberg, P.D., Selaru, P., Wilner, K.D., et al. (2010). A phase II study of PD-0325901, an oral MEK inhibitor, in previously treated patients with advanced non-small cell lung cancer. Clin. Cancer Res. *16*, 2450–2457.

Heidorn, S.J., Milagre, C., Whittaker, S., Nourry, A., Niculescu-Duvas, I., Dhomen, N., Hussain, J., Reis-Filho, J.S., Springer, C.J., Pritchard, C., and Marais, R. (2010). Kinase-dead BRAF and oncogenic RAS cooperate to drive tumor progression through CRAF. Cell *140*, 209–221.

Jackson, E.L., Olive, K.P., Tuveson, D.A., Bronson, R., Crowley, D., Brown, M., and Jacks, T. (2005). The differential effects of mutant p53 alleles on advanced murine lung cancer. Cancer Res. *65*, 10280–10288.

Jesenberger, V., Procyk, K.J., Ruth, J., Schreiber, M., Theussl, H.C., Wagner, E.F., and Baccarini, M. (2001). Protective role of Raf-1 in Salmonella-induced macrophage apoptosis. J. Exp. Med. *193*, 353–364.

Johnson, L., Mercer, K., Greenbaum, D., Bronson, R.T., Crowley, D., Tuveson, D.A., and Jacks, T. (2001). Somatic activation of the K-ras oncogene causes early onset lung cancer in mice. Nature *410*, 1111–1116.

Karnoub, A.E., and Weinberg, R.A. (2008). Ras oncogenes: split personalities. Nat. Rev. Mol. Cell Biol. *9*, 517–531.

Luo, J., Emanuele, M.J., Li, D., Creighton, C.J., Schlabach, M.R., Westbrook, T.F., Wong, K.K., and Elledge, S.J. (2009). A genome-wide RNAi screen identifies multiple synthetic lethal interactions with the Ras oncogene. Cell *137*, 835–848.

Malliri, A., and Collard, J.G. (2003). Role of Rho-family proteins in cell adhesion and cancer. Curr. Opin. Cell Biol. *15*, 583–589.

Malumbres, M., and Barbacid, M. (2003). RAS oncogenes: the first 30 years. Nat. Rev. Cancer *3*, 459–465.

Marshall, C.J. (1994). MAP kinase kinase kinase, MAP kinase kinase and MAP kinase. Curr. Opin. Genet. Dev. *4*, 82–89.

Matallanas, D., Romano, D., Yee, K., Meissl, K., Kucerova, L., Piazzolla, D., Baccarini, M., Vass, J.K., Kolch, W., and O'neill, E. (2007). RASSF1A elicits apoptosis through an MST2 pathway directing proapoptotic transcription by the p73 tumor suppressor protein. Mol. Cell *27*, 962–975.

Meylan, E., Dooley, A.L., Feldser, D.M., Shen, L., Turk, E., Ouyang, C., and Jacks, T. (2009). Requirement for NF-kappaB signalling in a mouse model of lung adenocarcinoma. Nature *462*, 104–107.

Mikula, M., Schreiber, M., Husak, Z., Kucerova, L., Rüth, J., Wieser, R., Zatloukal, K., Beug, H., Wagner, E.F., and Baccarini, M. (2001). Embryonic lethality and fetal liver apoptosis in mice lacking the c-raf-1 gene. EMBO J. *20*, 1952–1962.

Niault, T., Sobczak, I., Meissl, K., Weitsman, G., Piazzolla, D., Maurer, G., Kern, F., Ehrenreiter, K., Hamerl, M., Moarefi, I., et al. (2009). From autoinhibition to inhibition in trans: the Raf-1 regulatory domain inhibits Rok-alpha kinase activity. J. Cell Biol. *187*, 335–342.

Pagès, G., Guérin, S., Grall, D., Bonino, F., Smith, A., Anjuere, F., Auberger, P., and Pouysségur, J. (1999). Defective thymocyte maturation in p44 MAP kinase (Erk 1) knockout mice. Science *286*, 1374–1377.

Piazzolla, D., Meissl, K., Kucerova, L., Rubiolo, C., and Baccarini, M. (2005). Raf-1 sets the threshold of Fas sensitivity by modulating Rok-alpha signaling. J. Cell Biol. *171*, 1013–1022.

Poulikakos, P.I., Zhang, C., Bollag, G., Shokat, K.M., and Rosen, N. (2010). RAF inhibitors transactivate RAF dimers and ERK signalling in cells with wild-type BRAF. Nature *464*, 427–430.

Puyol, M., Martín, A., Dubus, P., Mulero, F., Pizcueta, P., Khan, G., Guerra, C., Santamaría, D., and Barbacid, M. (2010). A synthetic lethal interaction between K-Ras oncogenes and Cdk4 unveils a therapeutic strategy for non-small cell lung carcinoma. Cancer Cell *18*, 63–73.

Rinehart, J., Adjei, A.A., Lorusso, P.M., Waterhouse, D., Hecht, J.R., Natale, R.B., Hamid, O., Varterasian, M., Asbury, P., Kaldjian, E.P., et al. (2004). Multicenter phase II study of the oral MEK inhibitor, CI-1040, in patients with advanced non-small-cell lung, breast, colon, and pancreatic cancer. J. Clin. Oncol. *22*, 4456–4462.

Scholl, F.A., Dumesic, P.A., Barragan, D.I., Harada, K., Charron, J., and Khavari, P.A. (2009). Selective role for Mek1 but not Mek2 in the induction of epidermal neoplasia. Cancer Res. *69*, 3772–3778.

Simpson, A.J., Wallace, W.A., Marsden, M.E., Govan, J.R., Porteous, D.J., Haslett, C., and Sallenave, J.M. (2001). Adenoviral augmentation of elafin

protects the lung against acute injury mediated by activated neutrophils and bacterial infection. J. Immunol. *167*, 1778–1786.

Singh, A., Greninger, P., Rhodes, D., Koopman, L., Violette, S., Bardeesy, N., and Settleman, J. (2009). A gene expression signature associated with "K-Ras addiction" reveals regulators of EMT and tumor cell survival. Cancer Cell *15*, 489–500.

Takezawa, K., Okamoto, I., Yonesaka, K., Hatashita, E., Yamada, Y., Fukuoka, M., and Nakagawa, K. (2009). Sorafenib inhibits non-small cell lung cancer cell growth by targeting B-RAF in KRAS wild-type cells and C-RAF in KRAS mutant cells. Cancer Res. *69*, 6515–6521.

Tsai, J., Lee, J.T., Wang, W., Zhang, J., Cho, H., Mamo, S., Bremer, R., Gillette, S., Kong, J., Haass, N.K., et al. (2008). Discovery of a selective inhibitor of oncogenic B-Raf kinase with potent antimelanoma activity. Proc. Natl. Acad. Sci. USA *105*, 3041–3046.

Tuveson, D.A., Shaw, A.T., Willis, N.A., Silver, D.P., Jackson, E.L., Chang, S., Mercer, K.L., Grochow, R., Hock, H., Crowley, D., et al. (2004). Endogenous oncogenic K-ras(G12D) stimulates proliferation and widespread neoplastic and developmental defects. Cancer Cell *5*, 375–387.

Villanueva, J., Vultur, A., Lee, J.T., Somasundaram, R., Fukunaga-Kalabis, M., Cipolla, A.K., Wubbenhorst, B., Xu, X., Gimotty, P.A., Kee, D., et al. (2010). Acquired resistance to BRAF inhibitors mediated by a RAF kinase switch in melanoma can be overcome by cotargeting MEK and IGF-1R/PI3K. Cancer Cell *18*, 683–695.

Voice, J.K., Klemke, R.L., Le, A., and Jackson, J.H. (1999). Four human ras homologs differ in their abilities to activate Raf-1, induce transformation, and stimulate cell motility. J. Biol. Chem. *274*, 17164–17170.

Yamaguchi, O., Watanabe, T., Nishida, K., Kashiwase, K., Higuchi, Y., Takeda, T., Hikoso, S., Hirotani, S., Asahi, M., Taniike, M., et al. (2004). Cardiac-specific disruption of the c-raf-1 gene induces cardiac dysfunction and apoptosis. J. Clin. Invest. *114*, 937–943.